Analyst

Accepted Manuscript

This article can be cited before page numbers have been issued, to do this please use: X. Wei, X. Duan, X. Zhou, J. Wu, H. Xu, X. Min and S. Ding, *Analyst*, 2018, DOI: 10.1039/C8AN00549D.

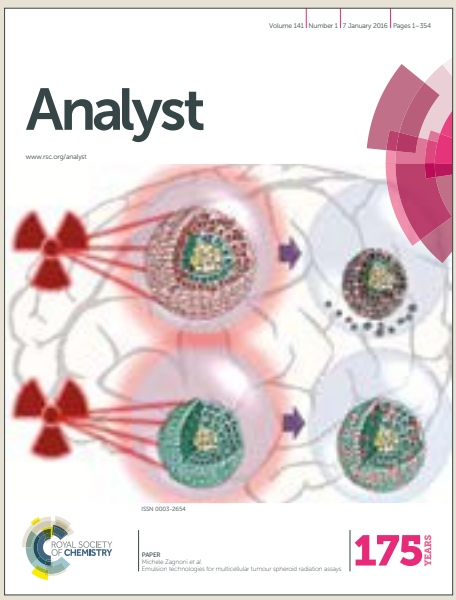

ROYAL SOCIETY OF CHEMISTRY

rsc.li/analyst

View Article Online
DOI: 10.1039/C8AN00549D

A highly sensitive SPRi biosensing strategy for simultaneous detection of multiplex miRNAs based on strand displacement amplification and AuNPs signal enhancement

Xiaotong Wei,[a,1] Xiaolei Duan,[a, b,1] Xiaoyan Zhou,[a] Jiangling Wu,[a] Hongbing Xu,[c] Xun Min,[b *] Shijia Ding[a *]

[a]*Key Laboratory of Clinical Laboratory Diagnostics (Ministry of Education), College of Laboratory Medicine, Chongqing Medical University, Chongqing 400016, China*

[b]*Department of Laboratory Medicine, The Affiliated Hospital of Zunyi Medical University, Zunyi, Guizhou 563000, China*

[c]*Department of Obstetrics and Gynecology, The First Affiliated Hospital of Chongqing Medical University, Chongqing 400016, China*

**Corresponding author; Email: dingshijia@163.com (S. Ding); Tel/Fax: +86-23-6 8485786. minxunzmu@163.com (X. Min); Tel/Fax: 0852-8608316.*

[1]*These authors contributed equally to this work.*

Abstract

Herein, a dual channel surface plasmon resonance imaging (SPRi) biosensor has been developed for simultaneous and highly sensitive detection of multiplex miRNAs based on strand displacement amplification (SDA) and DNA-functionalized AuNPs signal enhancement. In the presence of target miRNAs (miR-21 or miR-192), the miRNAs could specifically hybridize with the corresponding hairpin probes (H) and initiate the SDA, resulting in massive triggers. Subsequently, the two parts of the released triggers could hybridize with capture probes (CP) and DNA-functionalized AuNPs, assembling DNA sandwiches with great mass on the chip surface. A significantly amplified SPR signal readout was achieved. The established biosensing

View Article Online
DOI: 10.1039/C8AN00549D

method was capable of simultaneously detecting multiplex miRNAs with a limit of detection down to 0.15 pM for miR-21 and 0.22 pM for miR-192, respectively. The method exhibited good specificity and acceptable reproducibility. Moreover, the developed method was applied to the determination of target miRNAs in complex matrix. Thus, this developed SPRi biosensing method might present a potential alternative tool for miRNAs detection in biomedical research and clinical diagnosis.

Keywords: miRNAs, surface plasmon resonance imaging, DNA-functionalized AuNPs, strand displacement amplification.

1. Introduction

MicroRNAs (miRNAs), a class of conserved 19-23 nucleotide non-coding RNA, are known to be closely associated with the pathogenesis of human diseases, including acute kidney injury (AKI),[1] polycystic kidney disease (PKD)[2] and diabetic nephropathy (DN).[3-5] Several miRNAs, like miRNA-21 (miR-21) and miRNA-192 (miR-192), have been shown to play critical roles in DN due to their effects on key genes associated with DN.[5] Thus, simultaneous and accurate detection of multiplex miRNAs is helpful to elucidate the pathogenesis of DN for early clinical diagnosis, treatment and prevention.

The intrinsic characteristics of miRNAs, including short sequence, low concentrations of target miRNAs in analyzed samples, and sequence homology

View Article Online
DOI: 10.1039/C8AN00549D

among the miRNA family, pose a challenge for miRNA detection.[6] Accordingly, some conventional methods have been established to identify and quantify miRNAs, such as microarrays,[7] Northern blotting,[8] and quantitative reverse-transcription real-time polymerase chain reaction (qRT-PCR).[9] However, microarray and Northern blotting require complicated procedures, long assay time, and expensive reagents.[10] The qRT-PCR is sometimes limited by the use of locked nucleic acid (LNA)-modified primers or the optimization of sequence-specific annealing temperature.[6] Alternatively, several biosensing methods have been developed for miRNA analysis, such as electrochemistry,[11] electrochemiluminescence,[12] colorimetry,[13] fluorescence,[14] surface-enhanced Raman spectroscopy,[15] scanometric array profiling chip[16], photonic microring resonator[17, 18], surface plasmon resonance (SPR)[19, 20] and surface plasmon resonance imaging (SPRi).[21, 22] Among these biosensors, SPRi has been proven to be an attractive technology for simultaneous monitor of molecular interaction and quantitative detection of bio-molecular targets owing to its advantages of label-free, real-time, and high-throughput detection.[23]

In a typical SPR imaging system, a collimated, polarized and monochromatic light beam travels through a prism and an attached glass slide coated with gold film, and reflects from the gold/solution interface. The reflected light intensity is monitored at the specular angle by a charge-coupled device (CCD).[24] In this way, both sensorgrams (i.e., resonance signal vs time) and real-time images of the sensor chip can be simultaneously recorded for high-throughput analysis.[25] However, the sensitivity of SPRi biosensing method is not satisfying for direct detection of low

View Article Online
DOI: 10.1039/C8AN00549D

abundance biomolecules in complex matrix.[25] Also, the single polymorphisms in miRNA may cause false signals during the direct capture of miRNAs by standard capture probes[17], limiting its wide application.

Recently, aiming to enhance the sensitivity of SPRi biosensing method, a variety of amplified strategies have been developed for nucleic acids detection, including PCR,[26] enzyme catalysis amplification reaction,[27] enzyme-free amplification reaction,[19, 20] polymerization[21] and nanoparticle enhancement.[28, 29] In these amplification strategies, strand displacement amplification (SDA) has been received particular attention owing to its isothermal nature, high amplification efficiency, and rapid amplification kinetics.[10, 27] Meanwhile, various nanomaterials can also exhibit amplification efficiency for SPR and SPRi measurements, such as gold nanoparticles (AuNPs),[30, 31] SiO_2 nanoparticles,[32] quantum dots[33] and magnetic nanoparticles.[34] Significantly, AuNPs have been widely applied in SPR and SPRi biosensors for detection of biomolecules and show an excellent signal amplification performance,[28-30, 35] which exhibit good application prospect for implementation into a large range of SPR and SPRi measurements.[35, 36]

In this work, we developed a simple surface plasmon resonance imaging biosensor for simultaneous and sensitive detection of multiplex miRNAs by integrating SDA with DNA-functionalized AuNPs. The developed method exhibited highly sensitive detection of multiplex miRNAs due to the SDA signal amplification and DNA-functionalized AuNPs signal enhancement. In addition, this dual channel biosensing method enabled the simultaneous detection of multiplex miRNAs, which

View Article Online
DOI: 10.1039/C8AN00549D

might be a potential alternative tool for detection of multiplex miRNAs for early diagnosis, treatment, or prevention of DN.

2. Experimental section

2.1. Materials and reagents

Klenow fragment (3'-5'exo) was obtained from Thermo Fisher Scientific (Wilmington, USA). Nb.BbvCI and deoxyribonucleoside triphosphates (dNTPs) were purchased from New England Biolabs (Beijing, China). 6-Mercapto-1-hexanol (MCH) was purchased from Sigma-Aldrich (St. Louis, USA). Tris (2-carboxyethyl) phosphine (TCEP) was obtained from Aladdin Biochemical Technology Co., Ltd (Shanghai, China). $HAuCl_4 \cdot 4H_2O$ was purchased from Sinopharm Chem Co., Ltd (Shanghai, China). HPLC-purified miRNAs and DNA sequences, Triton X-100, bovine serum albumin (BSA), diethylpyrocarbonate (DEPC) were obtained from Sangon Biotechnology Co., Ltd (Shanghai, China). Fetal bovine serum was purchased from BBI Life Sciences Corporation (Shanghai, China). DNA Ladder Marker (20 bp) was obtained from TaKaRa (Dalian, China). Gelred nucleic acid stain was purchased from SenBeiJia Biological Technology Co., Ltd (Nanjing, China). All other reagents were of analytical grade. All aqueous solutions were prepared with ultrapure water by Millipore Milli-Q gradient ultrapure water system (Millipore, MA). The sequences of nucleic acids employed in this study were shown in Table S1. All oligonucleotides were dissolved in Tris-EDTA (TE) buffer (10 mM Tris-HCl, 1 mM EDTA, pH 8.0) and stored at -20 °C. To avoid miRNA degradation, all buffer solutions were treated

View Article Online
DOI: 10.1039/C8AN00549D

with DEPC by mixing 0.1% of DEPC with the solution.

2.2. Apparatus

A home-built SPRi platform and gold array sensor chips were used in the SPRi measurement. This home-built system was capable of simultaneously detecting bio-molecules in two separate flow cells with a volume of 50 μL (Image of dual channel SPRi was shown in Fig. S1). The gold sensor chips were fabricated with a 2 nm thick chromium adhesion layer, followed by deposition of a 46 nm thick gold layer via e-beam evaporation onto cleaned BK-7 glass slides. A red light emitting diode (LED, 650 nm) was used to excite the surface plasmon resonance near the metal surface. P-polarization of the light was obtained with a sheet polarizer. A refractive index matching liquid (n = 1.610) was mediated between the sensor chip and the high-refractive index prism (n = 1.616). The reflected images were captured by a cooled 12-bit CCD camera (Retiga 1300 from QImaging) with a resolution of 1.3 MP (1280 × 1024 pixels) and 6.7 μm × 6.7 μm pixel size. All experiments were carried out at an operating temperature of 25 ℃ ± 1 ℃. All sensorgrams were evaluated by a home-made program. Transmission electron microscopic (TEM) image was carried out on an H-7500 transmission electron microscope (Hitachi, Japan). The gel electrophoresis was performed on the DYY-6C electrophoresis analyzer (Liuyi Instrument Company, China) and imaged by a Bio-Rad ChemDoc XRS (Bio-Rad, USA). UV-visible spectra were carried out on a UV-2550 spectrophotometer (Shimadzu, Japan).

2.3. Preparation of AuNPs and DNA-functionalized AuNPs

View Article Online
DOI: 10.1039/C8AN00549D

AuNPs and DNA-functionalized AuNPs were prepared according to the literature.[37] Sodium citrate (10.1 mL, 34 mM) was added rapidly to boiling solution of $HAuCl_4$ (88.2 mL, 1 mM), and the color changed from pale yellow to deep red in 1 min. Then the resulting AuNPs solution was cooled to room temperature (23 - 25 ℃) with continued stirring for another 20 min and stored at 4 ℃ until use. The DNA-functionalized AuNPs were prepared by incubating a mixture consisting of 9 μL of 1 mM detection probes, 1 μL of 500 mM acetate buffer (pH 5.2) and 1.5 μL of 10 mM TCEP at room temperature for 1 h. Then the mixture was added into 3 mL of AuNPs solution, and the resulted solution was stored in a drawer at room temperature for at least 16 h. After that, 30 μL of 500 mM Tris-acetate buffer (500 mM, pH 8.2) was added dropwise to the mixture, and 300 μL of 1 M NaCl was added dropwise to the mixture. Subsequently, the resulting mixture was stored in a drawer for at least 12 h. Finally, the mixture was centrifuged at 12,000 rpm for 30 min to remove the excess reagents, and the red precipitate was washed, centrifuged and dispersed in running buffer for future use.

2.4. Probes immobilization on the sensor chip

The thiolated capture probes were immobilized on gold sensor chip of the different channels by the interaction of Au-S. Prior to modification, the gold sensor chip surface was firstly cleaned with fresh piranha solution (70% H_2SO_4, 30% H_2O_2) for 10 min to eliminate adsorbed organic impurities, following rinsed thoroughly with ultrapure water and finally dried under nitrogen. 200 μL of 1 μM thiolated capture probes in immobilization solution (1 M KH_2PO_4, pH 3.8) were carefully dropped onto

View Article Online
DOI: 10.1039/C8AN00549D

the pretreated gold sensor chip and incubated at 4 ℃ overnight. Followed washing with ultrapure water, the gold sensor chip was immersed into 1 mM MCH solution and 1% BSA for 1 h respectively, to block the nonspecific binding sites on gold sensor chip surface. After washing with ultrapure water, the gold sensor chip was dried by nitrogen and docked into the SPRi instrument for further experiment.

2.5. SDA reaction

SDA reactions were carried out in separate reaction tubes with 20 μL of total reaction volume consisting of 2 μL different miRNAs (miR-21 and miR-192, respectively) with various concentrations, 4 μL of 400 nM hairpin probes, 0.6 μL of 10 U/μL Klenow fragment, 0.6 μL of 10 U/μL Nb.BbvCI, 2 μL of 250 μM dNTP, 1.5 μL of 1.2 U/μL RNase inhibitor, 2 μL 10 × CutSmart™ buffer (20 mM pH 7.9 Tris-acetate, 500 mM potassium acetate, 10 mM magnesium acetate, 100 μg/mL BSA), 2 μL 10 × Klenow Fragment buffer (100 mM pH 7.5 Tris-HCl, 70 mM $MgCl_2$, 1 mM DTT) and 5.3 μL DEPC-treated water. Then the reaction tubes were incubated at 37 ℃ for 80 min.

2.6. Gel electrophoresis

To verify the feasibility of the SDA reaction, a 3% agarose gel electrophoresis analysis of the products was carried out in 1 × TBE buffer (90 mM Tris-HCl, 90 mM boric acid, 2 mM EDTA, pH 7.9) at 110 mV for about 38 min. The gel was photographed by Bio-Rad digital imaging system.

2.7. SPRi measurement

After the SDA reaction, the different resulting mixtures were incubated at 80 ℃

View Article Online
DOI: 10.1039/C8AN00549D

for 10 min to terminate the reaction, and diluted to 400 μL with running buffer (30 mM sodium phosphate, 450 mM NaCl, 3 mM EDTA, 0.25% Triton X-100, pH 7.4) for further experiment or stored at -20 °C. When the sensorgram reached a steady state, the diluted mixture solutions (400 μL) were respectively and simultaneously injected into the corresponding flow cell at the flow rate of 10 μL/min. After hybridization, the gold sensor chip was washed with the running buffer to reach a steady state. Then the DNA-functionalized AuNPs were respectively and simultaneously injected into the corresponding flow cell to form a DNA sandwich assembly at the flow rate of 10 μL/min. The gold sensor chip was regenerated with 50 mM NaOH to remove the bound analytes on the gold sensor chip for the next measurements. Three replicate tests were implemented and the average value was calculated. All experiments were carried out at room temperature about 25 °C.

3. Results and discussion

3.1. Principle of the SPRi biosensing method

The principle of SPRi biosensing method for multiplex miRNAs detection is shown in Scheme 1. The hairpin probe (H) consists of three domains, including a miRNA-recognition domain (H1 in blue, H2 in orange), an amplification domain (H1 and H2 both in yellow) as template to produce the triggers, and a recognition domain (H1 and H2 both in black) as nick site. The only structural difference between H1 and H2 is the miRNA-recognition domain. The same triggers will be produced by different SDA reaction initiated by miR-21 and miR-192. In the presence of miR-21 or miR-192, the miRNA specifically hybridizes with the recognition domain (H1 in

View Article Online
DOI: 10.1039/C8AN00549D

blue, H2 in orange) of hairpin probe and opens the loop region of hairpin probe. And the bound miRNA is extended along the hairpin probe to form a complete duplex with the aid of Klenow fragment polymerase and dNTPs. Subsequently, the Nb.BbvCI specifically recognizes the duplex nicking site (in black) and cleaves the extended DNA strand. Finally, the Klenow fragment polymerase can extend again along from the part of nick site, and the triggers (in red) will be displaced and released. Upon the circulation of the extension and cleavage processes, large amounts of triggers are released. Afterwards, the two parts of the released triggers can hybridize with capture probes (CP) and DNA-functionalized AuNPs, assembling DNA sandwiches with great mass on the chip surface. The amplified SPR signals in dual channels are simultaneously detected.

A typical sensorgram is shown in Fig. 1. ΔRU1 shows the response of duplex formation between the triggers and the capture probes. ΔRU2 shows the response of the DNA sandwich assembly between the DNA-functionalized AuNPs and the CP-trigger complexes. Therefore, the total response (ΔRU1 + ΔRU2) is associated with the massive triggers and the DNA-functionalized AuNPs enhancement.

3. 2. Feasibility of the proposed assay

The feasibility of the developed amplification strategy for multiplex miRNAs detection was evaluated and shown in Fig. 2. The AuNPs and the DNA-functionalized AuNPs were characterized and shown in Fig. S2. As shown in Fig. 2A/2C (curve a), in the absence of the miRNA, SDA could not be initiated to generate the triggers, resulting in a negligible SPR signal. On the contrary, with SDA amplification reaction,

View Article Online
DOI: 10.1039/C8AN00549D

only a small SPR signal was observed in Fig. 2A/2C (curve b). By comparison, the introduction of triggers generated by target-initiated SDA led to an increase of SPR signal, attributing to duplex formation between the triggers and the capture probes immobilized on the chip surface. With the addition of DNA-functionalized AuNPs, the SPR signal in Fig. 2A/2C (curve c) increased about 5 folds over control without AuNPs, which was attributed to the AuNPs effects, including the electromagnetic field coupling effect between LSPR-SPR, surface mass increase due to the size/mass-material properties of AuNPs and the refractive index change by the AuNPs.[36] These results clearly demonstrated the feasibility of the developed SPRi biosensing method for detection of multiplex miRNAs.

To further verify the validity of the SDA reaction, the triggers and the sequences of the SDA reaction were characterized by a 3% agarose gel electrophoresis analysis. As shown in Fig. 2B/2D, there was a distinct band near 20 bp, representing a large amount of triggers generated by SDA with the addition of miRNA (Fig. 2B/2D, lane 5). However, the band could not be observed in the control group without the addition of miRNA, indicating few SDA by-products were generated (Fig. 2B/2D, lane 4). These results clearly demonstrated that the SDA could be initiated in the presence of miRNA, effectively generating a large number of triggers.

3. 3. Optimization of the reaction conditions

Aiming to improve the performance of the SPRi biosensing strategy, the experiment conditions were systematically investigated. Hairpin probe acting as a template greatly affected the biosensing performance. As shown in Fig. 3A/3C, the

View Article Online
DOI: 10.1039/C8AN00549D

SPR signals increased with the increasing concentration of hairpin probes. The maximum signal was observed at the concentration of 80 nM. Therefore, 80 nM was chosen as the optimal concentration of each hairpin probes.

The reaction time was also of crucial importance for the SDA. As shown in Fig. 3B/3D, the signal increased with the increment of reaction time and reached the maximum at about 80 min and kept steady status. Hence, 80 min was chosen as the optimal reaction time.

3. 4. Analytical performance of miRNA detection

Under the optimal experimental conditions, the analytical performance of the developed method for multiplex miRNAs detection was investigated. As shown in Fig. 5A, the target miRNAs (miR-21 and miR-192, respectively) with increasing concentration from 0.5 pM to 500 pM led to gradual increase in the SPR signals. Fig. 5B showed a good relationship between the SPR signal and the miRNA concentrations in the range from 0.5 pM to 500 pM. Additionally, by plotting the concentration of miRNAs vs. SPR signal, the calibration curve over the range from 0.5 pM to 200 pM were obtained for miR-21 with a regression equation to be $y = 0.740 x + 5.948$ and a correlation coefficient of 0.993, for miR-192 with a regression equation to be $y = 0.736 x + 3.887$ and a correlation coefficient of 0.989 (Fig. 4B inset). The detection limit was evaluated to be 0.15 pM for miR-21 and 0.22 pM for miR-192, respectively. By comparison with other SPR and SPRi biosensing methods for miRNA detection (Table S2), this developed method showed high sensitivity for multiplex miRNAs detection. Such high sensitivity of the developed method could be

View Article Online
DOI: 10.1039/C8AN00549D

attributed to the high amplification efficiency of SDA as well as the LSPR-SPR coupling effect and the size/mass-material properties of AuNPs,[36] providing a highly sensitive detection strategy for multiplex miRNAs.

3.5. Specificity, reproducibility and reusability of the strategy

To investigate the specificity of the established SPRi biosensor, five different miRNA sequences, including target miRNA, single-base mismatched (SM), double-base mismatch (DM), non-complementary (NC) and miRNA-222 at the concentration of 100 pM were tested (miR-21 and miR-192, respectively). As shown in Fig. 5, the response signals of NC and miR-222 were similar to that of the blank. However, the presence of the target miRNA (miR-21 and miR-192, respectively) resulted in significantly increased response as compared with other miRNAs, indicating good specificity of the biosensor. In addition, five replicate tests were prepared for the detection of miR-21 and miR-192 at 100 pM. The relative standard deviations were 4.78% and 6.49%, respectively, suggesting good reproducibility of the method.

To further estimate the reusability of the biosensor, about 20 cycles of the binding/regeneration processes were carried on the same gold sensor chip, the SPR response decreased less than 10%, suggesting the cost effective and stable of the gold sensor chip. In addition, the procedure of the SPRi experiment was simple, which only needed two washing times with running buffer during the whole SPRi experiment (Table S3).

3.6. Recovery experiment

View Article Online
DOI: 10.1039/C8AN00549D

The application of the developed biosensing strategy for real samples was examined by detecting miRNAs in 10% diluted fetal bovine serum. Various concentrations of miRNAs were spiked into 10% diluted fetal bovine serum for detection, and the results showed the recovery of 104-110% for miR-21 and 103-108% for miR-192, respectively (Table S4), suggesting that the analytical performance of the biosensor was not significantly affected by complex matrix. Therefore, the developed biosensing method might provide a potential alternative tool for the detection of miRNAs in serum samples.

4. Conclusion

In conclusion, we developed a sensitive dual channel SPRi biosensor for simultaneous detection of multiplex miRNAs based on the SDA reaction and DNA-functionalized AuNPs. The high sensitivity of the method derived from the excellent signal amplification capability of SDA and the signal enhancement of DNA-functionalized AuNPs. The dual channel of the method also enabled the simultaneous detection of multiplex miRNAs. Additionally, this developed method showed good specificity and acceptable reproducibility. Moreover, this proposed method was applied for the detection of miRNAs in complex matrix. This established strategy presents a highly effective alternative platform for simultaneous detection of multiplex miRNAs, which may provide a potential tool for multiplex miRNAs in clinical diagnosis.

Acknowledgments

View Article Online
DOI: 10.1039/C8AN00549D

This work was funded by the National Natural Science Foundation of China (81572080, 81460317, and 31660241), the Special Project for Social Livelihood and Technological Innovation of Chongqing (cstc2016shmszx130043), and the Science and Technology Plan Project of Yuzhong District of Chongqing (20140121).

References

1. J. M. Lorenzen, T. Kaucsar, C. Schauerte, R. Schmitt, S. Rong, A. Hubner, K. Scherf, J. Fiedler, F. Martino, R. Kumarswamy, M. Kolling, I. Sorensen, H. Hinz, J. Heineke, E. van Rooij, H. Haller and T. Thum, *J. Am. Soc. Nephrol.*, 2014, **25**, 2717-2729.
2. V. Patel, D. Williams, S. Hajarnis, R. Hunter, M. Pontoglio, S. Somlo and P. Igarashi, *Proc. Natl. Acad. Sci. U. S. A.*, 2013, **110**, 10765-10770.
3. B. N. Chau, C. Xin, J. Hartner, S. Ren, A. P. Castano, G. Linn, J. Li, P. T. Tran, V. Kaimal, X. Huang, A. N. Chang, S. Li, A. Kalra, M. Grafals, D. Portilla, D. A. MacKenna, S. H. Orkin and J. S. Duffield, *Sci. Transl. Med.*, 2012, **4**, 121ra118.
4. M. Kato, J. Zhang, M. Wang, L. Lanting, H. Yuan, J. J. Rossi and R. Natarajan, *Proc. Natl. Acad. Sci. U. S. A.*, 2007, **104**, 3432-3437.
5. K. Bhatt, M. Kato and R. Natarajan, *Am. J. Physiol. Renal Physiol.*, 2016, **310**, F109-118.
6. W. Lu, Y. Chen, Z. Liu, W. Tang, Q. Feng, J. Sun and X. Jiang, *ACS Nano*, 2016, **10**, 6685-6692.
7. M. Castoldi, S. Schmidt, V. Benes, M. W. Hentze and M. U. Muckenthaler, *Nat. Protoc.*, 2008, **3**, 321-329.
8. M. de Planell-Saguer, M. C. Rodicio and Z. Mourelatos, *Nat. Protoc.*, 2010, **5**, 1061-1073.
9. C. Chen, D. A. Ridzon, A. J. Broomer, Z. Zhou, D. H. Lee, J. T. Nguyen, M. Barbisin, N. L. Xu, V. R. Mahuvakar, M. R. Andersen, K. Q. Lao, K. J. Livak and K. J. Guegler, *Nucleic Acids Res.*, 2005, **33**, e179.
10. Y. Zhao, F. Chen, Q. Li, L. Wang and C. Fan, *Chem. Rev.*, 2015, **115**, 12491-12545.
11. Z. Gao, *Analyst*, 2012, **137**, 1674-1679.
12. Y. Cheng, J. Lei, Y. Chen and H. Ju, *Biosens. Bioelectron.*, 2014, **51**, 431-436.
13. Y. Yan, B. Shen, H. Wang, X. Sun, W. Cheng, H. Zhao, H. Ju and S. Ding, *Analyst*, 2015, **140**, 5469-5474.
14. F. Causa, A. Aliberti, A. M. Cusano, E. Battista and P. A. Netti, *J. Am. Chem. Soc.*, 2015, **137**, 1758-1761.
15. L. P. Ye, J. Hu, L. Liang and C. Y. Zhang, *Chem. Commun. (Camb.)*, 2014, **50**, 11883-11886.
16. A. H. Alhasan, D. Y. Kim, W. L. Daniel, E. Watson, J. J. Meeks, C. S. Thaxton and C. A. Mirkin, *Anal. Chem.*, 2012, **84**, 4153-4160.
17. A. J. Qavi and R. C. Bailey, *Angew. Chem. Int. Ed. Engl.*, 2010, **49**, 4608-4611.
18. A. J. Qavi, J. T. Kindt, M. A. Gleeson and R. C. Bailey, *Anal. Chem.*, 2011, **83**, 5949-5956.
19. X. Ding, W. Cheng, Y. Li, J. Wu, X. Li, Q. Cheng and S. Ding, *Biosens. Bioelectron.*, 2017, **87**, 345-351.
20. X. Li, W. Cheng, D. Li, J. Wu, X. Ding, Q. Cheng and S. Ding, *Biosens. Bioelectron.*, 2016, **80**, 98-104.

View Article Online
DOI: 10.1039/C8AN00549D

21. F. Hu, J. Xu and Y. Chen, *Anal. Chem.*, 2017, **89**, 10071-10077.
22. S. Fang, H. J. Lee, A. W. Wark and R. M. Corn, *J. Am. Chem. Soc.*, 2006, **128**, 14044-14046.
23. J. B. Fasoli and R. M. Corn, *Langmuir*, 2015, **31**, 9527-9536.
24. C. T. Campbell and G. Kim, *Biomaterials*, 2007, **28**, 2380-2392.
25. J. Wu, Y. Huang, X. Bian, D. Li, Q. Cheng and S. Ding, *Opt. Commun.*, 2016, **377**, 24-32.
26. R. Wang, M. Minunni, S. Tombelli and M. Mascini, *Biosens. Bioelectron.*, 2004, **20**, 598-605.
27. K. Zeng, H. Li and Y. Peng, *Microchimica Acta*, 2017, **184**, 2637-2644.
28. Q. Wang, Q. Li, X. Yang, K. Wang, S. Du, H. Zhang and Y. Nie, *Biosens. Bioelectron.*, 2016, **77**, 1001-1007.
29. W. Hu, G. He, H. Zhang, X. Wu, J. Li, Z. Zhao, Y. Qiao, Z. Lu, Y. Liu and C. M. Li, *Anal. Chem.*, 2014, **86**, 4488-4493.
30. H. Vaisocherova, H. Sipova, I. Visova, M. Bockova, T. Springer, M. L. Ermini, X. Song, Z. Krejcik, L. Chrastinova, O. Pastva, K. Pimkova, M. Dostalova Merkerova, J. E. Dyr and J. Homola, *Biosens. Bioelectron.*, 2015, **70**, 226-231.
31. R. Liu, Q. Wang, Q. Li, X. Yang, K. Wang and W. Nie, *Biosens. Bioelectron.*, 2017, **87**, 433-438.
32. W. J. Zhou, Y. Chen and R. M. Corn, *Anal. Chem.*, 2011, **83**, 3897-3902.
33. A. M. Foudeh, J. T. Daoud, S. P. Faucher, T. Veres and M. Tabrizian, *Biosens. Bioelectron.*, 2014, **52**, 129-135.
34. J. Wang, A. Munir, Z. Zhu and H. S. Zhou, *Anal. Chem.*, 2010, **82**, 6782-6789.
35. V. Amendola, R. Pilot, M. Frasconi, O. M. Marago and M. A. Iati, *J Phys Condens Matter*, 2017, **29**, 203002.
36. X. Hong and E. A. Hall, *Analyst*, 2012, **137**, 4712-4719.
37. J. Liu and Y. Lu, *Nat. Protoc.*, 2006, **1**, 246-252.

View Article Online
DOI: 10.1039/C8AN00549D

Figure Captions

Scheme 1. Schematic representation of multiplex miRNAs SPRi biosensor.

Fig. 1. Typical SPR sensorgram of the triggers hybridization and DNA-functionalized AuNPs signal enhancement.

Fig. 2. (A/C) SPR sensorgrams corresponding to blank SDA-21/blank SDA-192 (curve a), SDA-21/SDA-192 (curve b) and SDA-21/SDA-192 combined with DNA-functionalized AuNPs (curve c). (B/D) The gel electrophoresis results of SDA. DNA ladder markers (lane 1), miRNA-21 /miRNA-192 (lane 2), H1/H2 (lane 3), blank SDA-21/blank SDA-192 (lane 4) and SDA-21 /SDA-192 (lane 5).

Fig. 3. Optimization of experimental parameters. Evaluation of (A) the effect of the concentration of H1, (B) the reaction time of SDA-21, (C) the effect of concentration of H2, (D) the reaction time of SDA-192. All data expressed as mean ± standard variation (n = 3).

Fig. 4. (A) SPR sensorgrams for detection of miRNAs at 0.5, 2, 5, 10, 50, 100, 200, 300, 500 pM (from a to i). (B) The calibration curve of the designed strategy for miR-21 and miR-192. All data expressed asmean ± standard variation (n = 3).

Fig. 5. SPR sensorgrams and SPR signal response (inset) respectively corresponding to various oligonucleotides (100 pM), (a) target miRNA, (b) SM, (c) DM, (d) NC, (e) miR-222, and (f) blank (A: miR-21, B: miR-192, respectively). All data expressed as mean ± standard variation (n = 3).

View Article Online
DOI: 10.1039/C8AN00549D

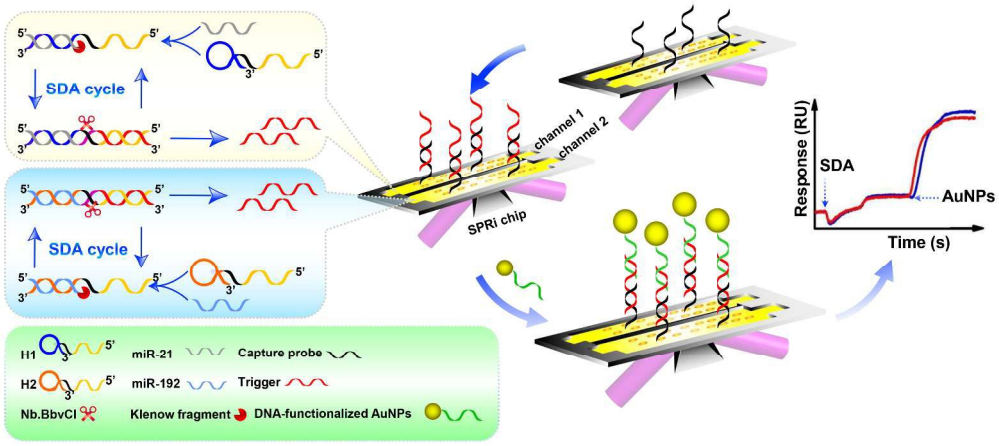

Scheme 1. Schematic representation of multiplex miRNAs SPRi biosensor.

300x132mm (300 x 300 DPI)

View Article Online
DOI: 10.1039/C8AN00549D

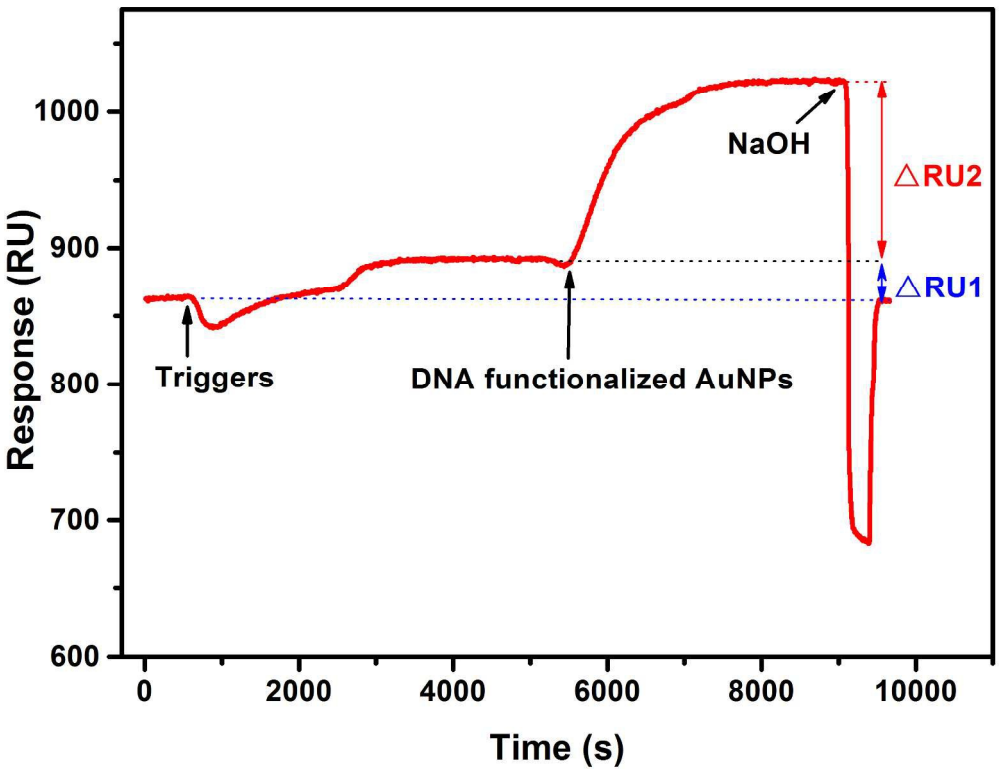

Fig. 1. Typical SPR sensorgram of the triggers hybridization and DNA-functionalized AuNPs signal enhancement.

232x180mm (300 x 300 DPI)

View Article Online
DOI: 10.1039/C8AN00549D

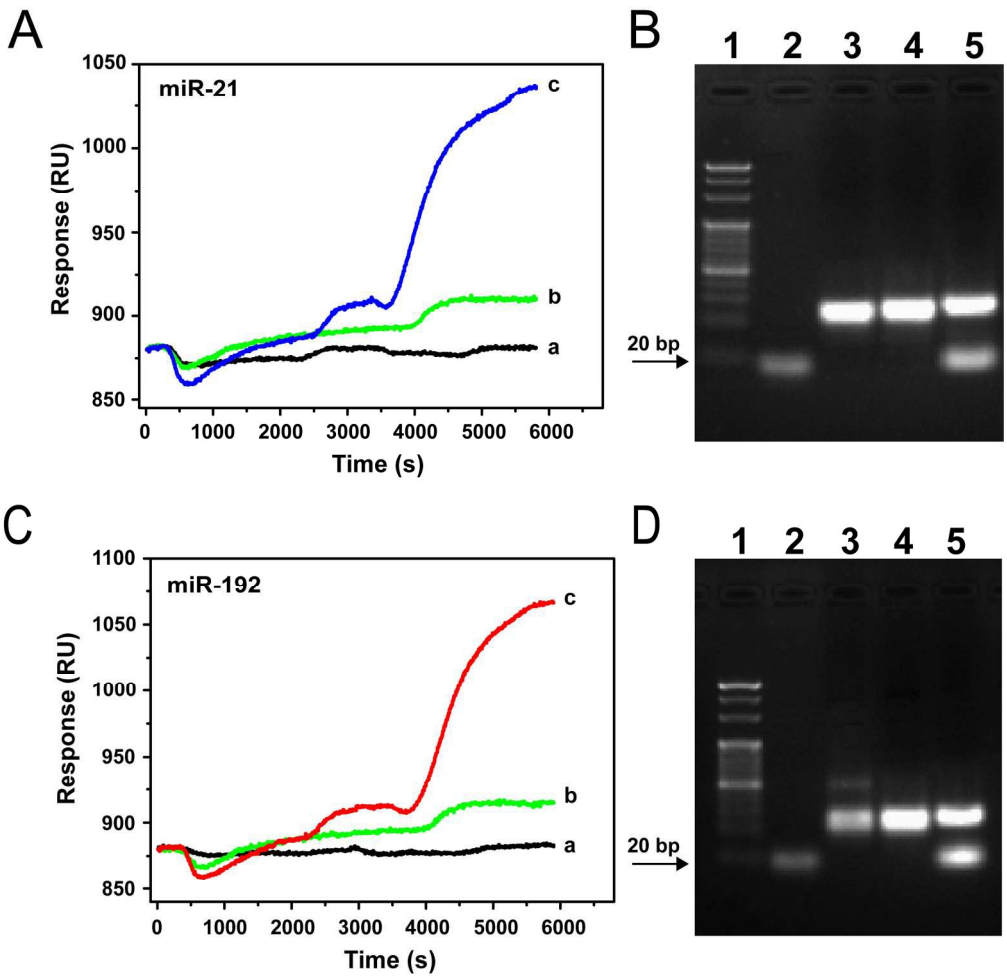

Fig. 2. (A/C) SPR sensorgrams corresponding to blank SDA-21/blank SDA-192 (curve a), SDA-21/SDA-192 (curve b) and SDA-21/SDA-192 combined with DNA-functionalized AuNPs (curve c). (B/D) The gel electrophoresis results of SDA. DNA ladder markers (lane 1), miRNA-21 /miRNA-192 (lane 2), H1/H2 (lane 3), blank SDA-21/blank SDA-192 (lane 4) and SDA-21 /SDA-192 (lane 5).

175x171mm (300 x 300 DPI)

View Article Online
DOI: 10.1039/C8AN00549D

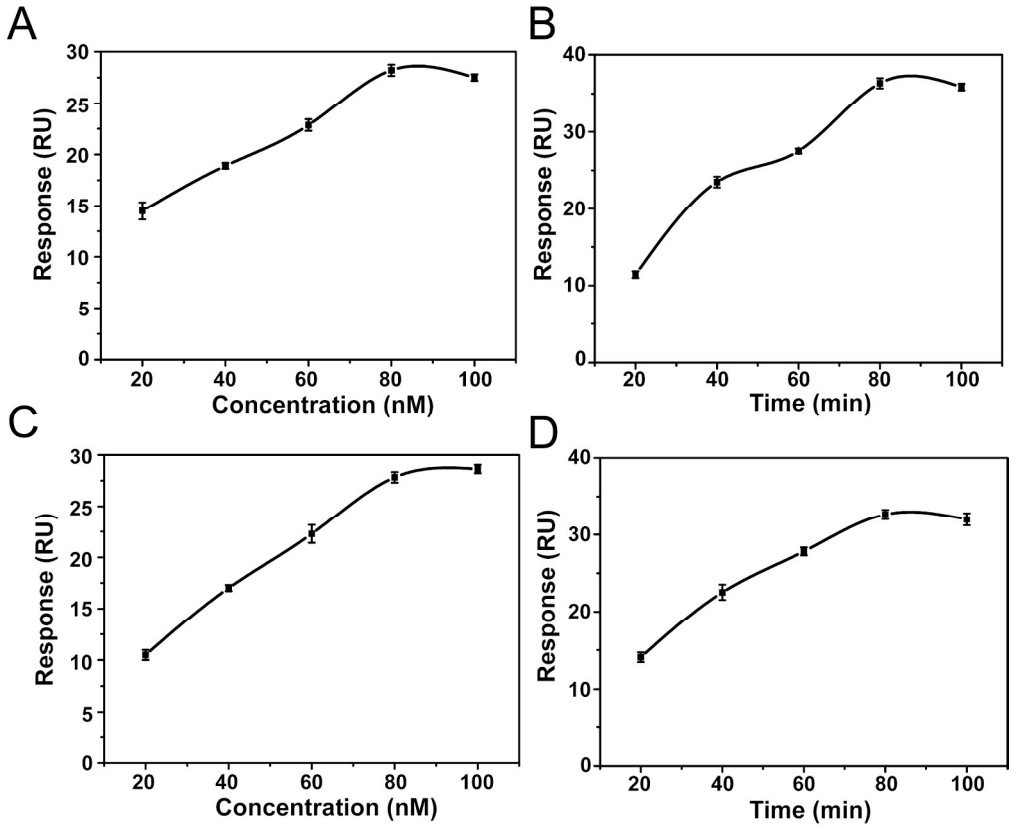

Fig. 3. Optimization of experimental parameters. Evaluation of (A) the effect of the concentration of H1, (B) the reaction time of SDA-21, (C) the effect of concentration of H2, (D) the reaction time of SDA-192. All data expressed as mean ± standard variation (n = 3).

203x168mm (300 x 300 DPI)

View Article Online
DOI: 10.1039/C8AN00549D

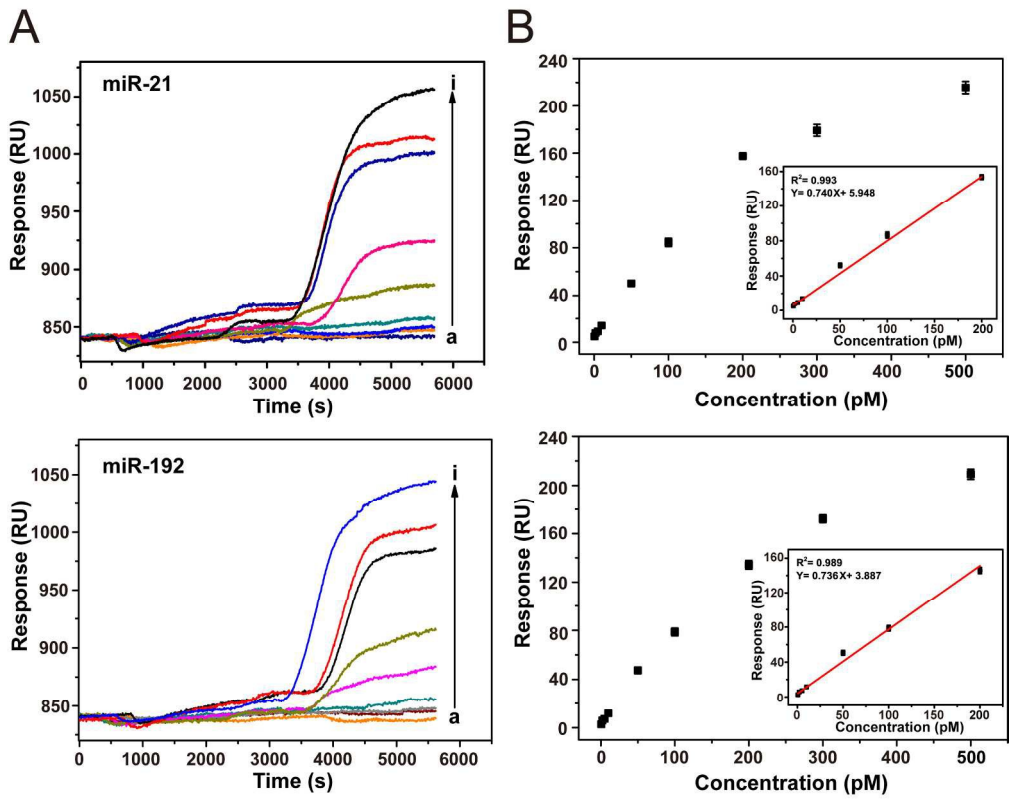

Fig. 4. (A) SPR sensorgrams for detection of miRNAs at 0.5, 2, 5, 10, 50, 100, 200, 300, 500 pM (from a to i). (B) The calibration curve of the designed strategy for miR-21 and miR-192. All data expressed asmean ± standard variation (n = 3).

200x159mm (300 x 300 DPI)

View Article Online
DOI: 10.1039/C8AN00549D

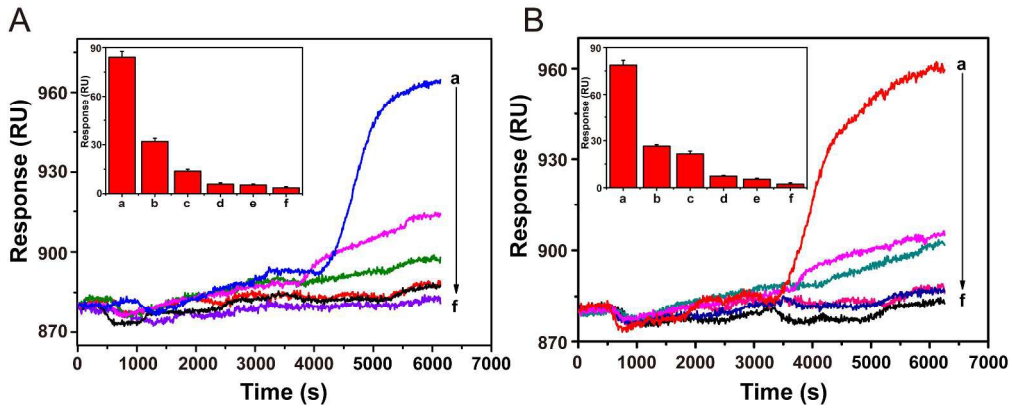

Fig. 5. SPR sensorgrams and SPR signal response (inset) respectively corresponding to various oligonucleotides (100 pM), (a) target miRNA, (b) SM, (c) DM, (d) NC, (e) miR-222, and (f) blank (A: miR-21, B: miR-192, respectively). All data expressed as mean ± standard variation (n = 3).

277x112mm (300 x 300 DPI)